



High-performance green phosphorescent top-emitting organic light-emitting diodes based on FDTD optical simulation

Xindong Shi^a, Jing Wang^a, Jun Liu^a, Saijun Huang^a, Xinkai Wu^a, Chaoping Chen^a,
Jiangang Lu^a, Yikai Su^a, Youxuan Zheng^{b,*}, Woo Young Kim^c, Gufeng He^{a,*}

^a National Engineering Lab for TFT-LCD Materials and Technologies, Department of Electronic Engineering, Shanghai Jiao Tong University, Shanghai 200240, People's Republic of China

^b State Key Laboratory of Coordination Chemistry, Nanjing National Laboratory of Microstructures, School of Chemistry and Chemical Engineering, Nanjing University, Nanjing 210093, People's Republic of China

^c Department of Green Energy & Semiconductor Engineering, Hoseo University, Asan, South Korea

ARTICLE INFO

Article history:

Received 8 November 2013

Received in revised form 21 December 2013

Accepted 15 January 2014

Available online 10 February 2014

Keywords:

Organic light-emitting diodes (OLEDs)

Low efficiency roll-off

Top-emitting

FDTD

ABSTRACT

We have successfully applied finite-difference time-domain (FDTD) method in top-emitting organic light-emitting diodes (TOLEDs) for structure optimization, demonstrating good agreement with experimental data. A mixed host with both hole transport and electron transport materials is employed for the green phosphorescent emitter to avoid charge accumulation and broaden the recombination zone. The resulting TOLEDs exhibit ultra-high efficiencies, low current efficiency roll-off, and a highly saturated color, as well as hardly detectable spectrum shift with viewing angles. In particular, a current efficiency of 127.0 cd/A at a luminance of 1000 cd/m² is obtained, and maintains to 116.3 cd/A at 10,000 cd/m².

© 2014 Elsevier B.V. All rights reserved.

1. Introduction

Interest in next-generation displays technologies has stimulated research on active-matrix organic light-emitting diodes (AMOLEDs) [1,2]. In the design of AMOLEDs, the top-emitting structure permitting the light to emit through the top electrode is preferred due to its favorable merits, such as high aperture ratio, high pixel resolution, and low power consumption. This is desirable for AMOLEDs with underneath wirings and transistors [3,4].

Recently, many efforts have been made to improve the performance of TOLEDs. And most of them focused on adopting a classical analytic method to design device

structures and various interface modifications to improve both optimum optical characteristics and electrical properties [5,6]. However, the classical analytic method is no longer applicable for the comparatively complex structure, while finite-difference time-domain (FDTD) method is a powerful simulation tool for complex OLED designs since this method is virtually applicable to any type of structure [7]. Additionally, phosphorescent light-emitting materials were widely used to improve the efficiencies of OLEDs since they can use triplet excitons for light emission and have a theoretical maximum internal quantum efficiency of 100% [8,9]. Nevertheless, since the triplet excitons will self-quench through triplet-triplet annihilation (TTA) or triplet-polaron annihilation (TPA) at high excitons densities, it is still a significant challenge to maintain a relative high efficiency at high luminance [10]. For example, Najafabadi et al. [11] reported a highly efficient green-phosphorescent top-emitting OLED with a current efficiency of 94 cd/A at a luminance of 1000 cd/m², but it

* Corresponding author. Address: 800 DongChuan Rd, Shanghai 200240, People's Republic of China. Tel.: +86 21 3420 7045; fax: +86 21 3420 4371.

E-mail addresses: yxzheng@nju.edu.cn (Y. Zheng), gufenghe@sjtu.edu.cn (G. He).

dropped to 76 cd/A at 10,000 cd/m². In 2013, the same group further published an inverted top-emitting phosphorescent OLED with a current efficiency of 110 cd/A at 1000 cd/m² by adopting a novel Ag/HAT-CN/TAPC anode structure [12]. However, the spectra changed a lot over different viewing angles, which is a serious problem for display application. It is still a big challenge to fulfill all these requirements.

In this paper, we present high-performance green top-emitting phosphorescent OLEDs with a simplified tri-layer structure. The optical properties, such as spectra, relative outcoupling efficiencies, and angular distribution profile predicted by FDTD simulation are in good agreement with the experimental results, showing that FDTD is a powerful simulation tool for TOLED. By optical and electrical optimization, the devices with a highly saturated color and weak angle dependence have been realized. Furthermore, the optimized device achieves a high current efficiency of 127.0 cd/A at a luminance of 1000 cd/m², and maintains to 116.3 cd/A at 10,000 cd/m², which is 2.7 times as high as that of traditional bottom-emitting OLED (BOLED).

2. Experimental

Substrates of glass were cut into 2.5 × 2.5 cm² squares and were cleaned successively using detergent, acetone, and isopropanol in an ultrasonic bath. The substrates were treated for 15 min in each solvent and then blown dry with nitrogen gas. Then, a 150-nm-thick patterned Al layer was deposited onto the glass substrates as an anode in a high-vacuum electron beam evaporation system under a base of below 3 × 10⁻⁵ Torr. The samples were then transferred to a vacuum thermal evaporator and the chamber was pumped down to a base pressure of 5 × 10⁻⁵ Torr. A 3-nm-thick MoO₃ was first deposited on patterned Al coated glass substrates followed by all organic layers which were subsequently deposited at a rate of 0.5–1 Å/s.

The detailed device (Device A, B, C) structures are depicted in Fig. 1, where 1,3-bis(carbazol-9-yl)benzene (mCP) is as the hole transport layer (HTL), as well as light emitting host. 4,4'-bis(N-(1-naphthyl)-N-phenyl-amino) biphenyl (NPB) is another kind of hole transport material, while 4,7-diphenyl-1,10-phenanthroline (Bphen) is as the electron transport layer (ETL). 1,3,5-tris(N-phenylbenzimidazole-2-yl)benzene (TPBi) is a light emitting host

material with predominant electron transport property, and iridium(III)bis(2-(4-trifluoromethylphenyl)pyridine) tetraphenylimidodiphosphinate (Ir(tfmppy)₂(tpip)) [13] is a green phosphorescent dye and as the emission layer (EML). The doping concentration of Ir(tfmppy)₂(tpip) in mCP and co-host is 6 wt% and the ratio of mCP:TPBi in co-host is 1:1 in device C. MoO₃ (3 nm) and the bi-layer structure 8-hydroxyquinoline lithium (Liq) (1 nm)/Al (1 nm) are utilized as hole and electron injection layer, respectively. To extract additional light from the devices and achieve both appropriate reflectivity and low absorption of the top contact for major emission wavelength of Ir(tfmppy)₂(tpip), an 80-nm-thick capping layer (CL) of mCP was deposited on top of the Ag. Fig. 2 shows the molecular structure of Ir(tfmppy)₂(tpip) and the energy level diagram extracted from the literatures [13–15].

The current density–voltage–luminance characteristics were measured by a computer controlled Keithley 2400 programmable voltage–current source and Topcon BM-7A Luminance Colorimeter. The emission spectra at different angles were measured with a calibrated Labsphere CDS 610 spectrometer by placing the TOLEDs on a rotating stage. All the measurements were carried out at the room temperature under ambient atmosphere.

3. Results and discussion

For effective design of devices, we have simulated the light emission profile using FDTD method, which allows for calculation of broad band emission in one run [7]. To match the random orientation and emission behavior of evaporated small molecules, we set three independent orthogonal dipoles and averaged the intensities in air. Fig. 3(a) sketches the cross section of BOLED and TOLED studied here. In the simulation, the refractive indices of organic materials and glass were assumed to be 1.77 and 1.51 over the wavelength of interest, respectively [16]. The complex refractive indices of the metallic electrodes and indium tin oxide (ITO) were taken from Refs. [17] and [18], respectively. We achieve an optimized configuration of optics for the TOLEDs shown in Fig. 1 via varying the length of the cavity and the location of the active layer in FDTD simulation. Fig. 3(c and d) shows the emission profiles of BOLEDs and TOLEDs calculated by FDTD, respectively, in which the TOLEDs' spectral radiance energy is

mCP (80 nm)	mCP (80 nm)	mCP (80 nm)
Liq (1 nm)/Al (1 nm)/ Ag (22 nm)	Liq (1 nm)/Al (1 nm)/ Ag (22 nm)	Liq (1 nm)/Al (1 nm)/ Ag (22nm)
Bphen (55 nm)	Bphen (55 nm)	Bphen (55 nm)
mCP: Ir(tfmppy) ₂ (tpip) (15 nm)	mCP: Ir(tfmppy) ₂ (tpip) (15 nm)	mCP:TPBi: Ir(tfmppy) ₂ (tpip) (15 nm)
NPB (40 nm)	mCP (40 nm)	mCP (40 nm)
Al/MoO ₃ (3 nm)	Al/MoO ₃ (3 nm)	Al/MoO ₃ (3 nm)
Glass	Glass	Glass
Device A	Device B	Device C

Fig. 1. Schematic device structures in this study.

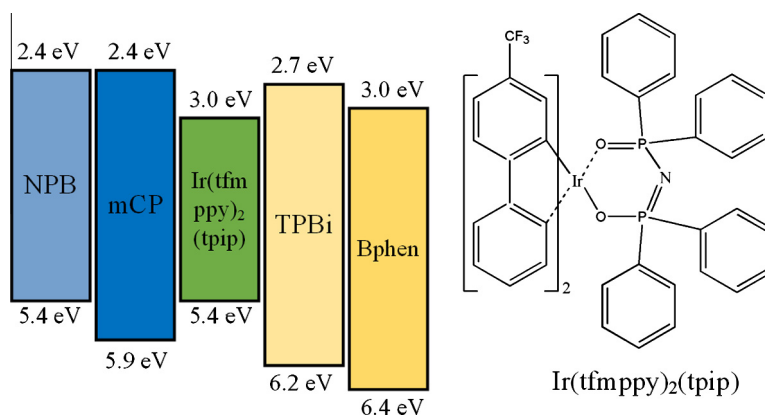


Fig. 2. Energy level diagram and chemical structure of Ir(tfmpppy)₂(tpip).

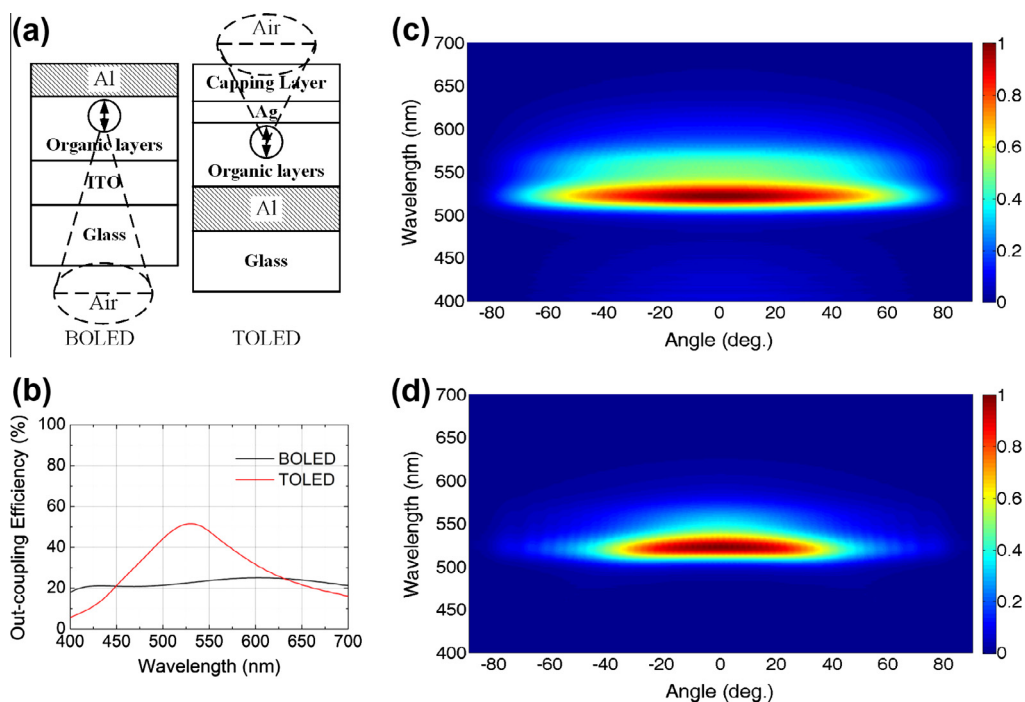


Fig. 3. (a) Schematic depicting the BOLED and TOLED structures; (b) FDTD simulation of out coupling efficiency, and angle- and wavelength-dependent normalized emission intensities of the (c) BOLED and (d) TOLED, respectively.

more concentrated than BOLED. Furthermore, we obtain the out-coupling efficiency by calculating the ratio between the fraction of the power transmitted into the air and the total radiated power of a dipole source. It is observed in Fig. 3(b) that the TOLED has significantly enhanced light out-coupling efficiency, from 21% to 51% at the wavelength of 522 nm, compared with BOLED.

On the basis of FDTD simulation, TOLED devices were fabricated satisfying microcavity resonance with a basic structure of glass/Al (150 nm)/MoO₃ (3 nm)/HTL (40 nm)/EML (15 nm)/ETL (55 nm)/Liq (1 nm)/Al (1 nm)/Ag (22 nm)/CL (80 nm). For comparison, a BOLED with the same layer structure of device C was also fabricated, except

that the 150-nm-thick Al anode was replaced by a 100-nm-thick ITO, and the 22-nm-thick semitransparent Ag cathode was replaced by Al (100 nm).

Fig. 4(a) shows that the measured electroluminescent (EL) spectrum of the TOLED is in good agreement with the simulated one, confirming the accuracy of FDTD simulation. Because of the microcavity effects, the TOLED exhibits a narrower EL spectrum with a full width at half maximum (FWHM) of 25 nm, in comparison with that of 58 nm for the BOLED. The Commission Internationale d'Eclairage (CIE) chromaticity coordinates of TOLED are (0.27, 0.67) at normal direction, which are obviously more saturated than of BOLED, as shown in Fig. 4(b). Moreover, it

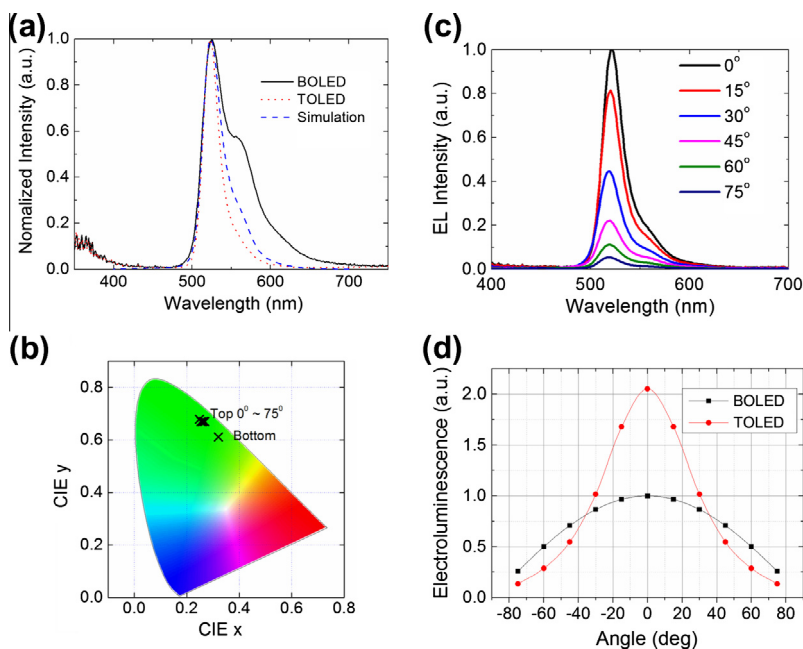


Fig. 4. Simulated and measured EL spectra (normalized) of the optimized TOLED and the corresponding BOLED at the normal direction; (b) CIE color coordinates of the TOLED from 0° to 75° and the BOLED at normal direction; (c) EL spectra with relative intensities measured at different viewing angles of TOLEDs; (d) normalized EL intensity distribution over viewing angles.

is clearly observed in Fig. 4(c) that the peak wavelengths do not shift when the viewing angle increases from 0° to 75°, and the color coordinates keep almost constant from 0° to 60°, and only slight shifts are observed at 75° with color coordinates of (0.25, 0.68). This means that the angular dependence of the color and the EL spectra of TOLEDs can be significantly suppressed by a properly tuned resonant cavity length and an antireflection capping layer [19], which may be applied to other emitting materials as well. In addition, Fig. 4(d) compares the angular distribution characteristics of TOLED and BOLED, in which the integrated light intensities are normalized to the light intensity of BOLED at normal direction. The TOLED exhibits a non-Lambertian emission pattern and significantly enhanced emission from 0° to 35° due to microcavity effect. The total emission power is much larger than that of BOLED. Such characteristics are laudable for small- or medium-size OLED display applications, which mainly concern the forward directed emission.

Fig. 5(a) compares the current density–voltage (I – V) characteristics of device A, B, and C. The highest occupied molecular orbital (HOMO) level of NPB is between the work function of Al and mCP, it was expected that the intermediate energy step can facilitate the hole injection. However, higher current density was observed when NPB was replaced by mCP instead. It indicates that the MoO₃ injection layer provides direct hole injection into mCP already [20], while the distinct energy barrier between NPB and mCP hinders the hole injection from NPB to mCP, resulting in holes accumulation at the interface. By adding electron transport host into the emission layer, the device C shows slightly higher current density at low voltage

range, which may be attributed to better electron transport from Bphen ETL to EML. Fig. 5(b) depicts the current efficiency curves versus luminance of device A, B, C, and BOLED. The device C exhibits a current efficiency of 99.8 cd/A at 1000 cd/m², around 2.1 times as high as 46.1 cd/A achieved by non-cavity BOLED, further confirming the accuracy of the FDTD simulation for out-coupling efficiency, as illustrated in Fig. 3(b). Furthermore, the efficiency of device C is superior to device B (85.9 cd/A), and device A (80.8 cd/A), indicating that the co-host in EML greatly improves the carrier balance of device. More importantly, the utilization of co-host structure significantly suppresses the efficiency roll-off at high luminance. Table 1 summarizes the device performances in detail. The current efficiency of device C is slightly reduced from 99.8 cd/A at 1000 cd/m² to 91.0 cd/A at 10,000 cd/m², with a roll-off of only 8.8%. In contrast, 31.9% efficiency roll-off for device A and 18.2% for device B are found, respectively. It has been well known that the accumulation of holes at the interface of HTL/EML and the narrow recombination zone were inferior for the efficiency roll-off due to TTA and TPA processes [21]. Here, the device C, using mCP as the hole transport layer and utilizing mCP and TPBi as the co-host, not only eliminates the accumulation of holes at the interface of NPB/EML, but also broadens the exciton-formation region and balances the charge injection and transport [22].

These results demonstrate that using co-host system and optimized optical microcavity structure can lead to high performance phosphorescent TOLEDs. In addition, the Al/MoO₃ reflective anode injects holes directly into the HOMO of the mCP host (5.9 eV) without requiring an

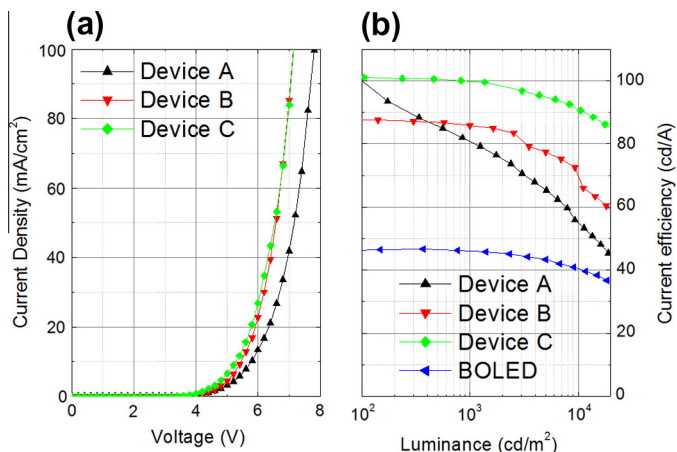


Fig. 5. (a) Current density–voltage and (b) current efficiency–luminance characteristics of device A, B, and C.

Table 1

Performance parameters of device A, B and C.

Devices	Current efficiency (cd/A)		Efficiency roll-off (%) (1000–10,000 cd/m ²)
	1000 cd/m ²	10,000 cd/m ²	
A	80.8	55.0	31.90%
B	85.9	70.2	18.20%
C	99.8	91.0	8.80%

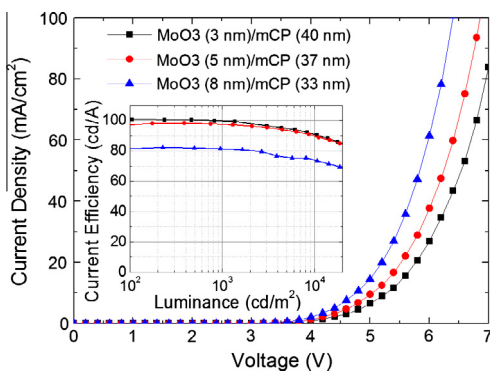


Fig. 6. Current density versus voltage of the device C with different thickness of MoO₃ as a hole injection layer and current efficiency versus luminance as an inset.

additional hole transport material with an intermediate HOMO level. Using mCP as a hole transport layer has the additional benefits of reducing the number of different materials needed and eliminating an organic–organic heterojunction of dissimilar materials [11,22].

To further optimize the charge carrier balance of the device, the thickness of MoO₃ injection layer has been varied to investigate its effects on hole injection capability from the anode. A series of devices structure consisted of Glass/Al (150 nm)/MoO₃ (x nm, $x = 3, 5, 8$ nm)/mCP (y nm, $y = 40, 37, 33$ nm)/mCP:TPBi:Ir(tfmpppy)₂(tpip) (6 wt%, 15 nm)/Bphen (55 nm)/LiQ (1 nm)/Al (1 nm)/Ag (22 nm)/mCP (80 nm) were fabricated, keeping the total optical

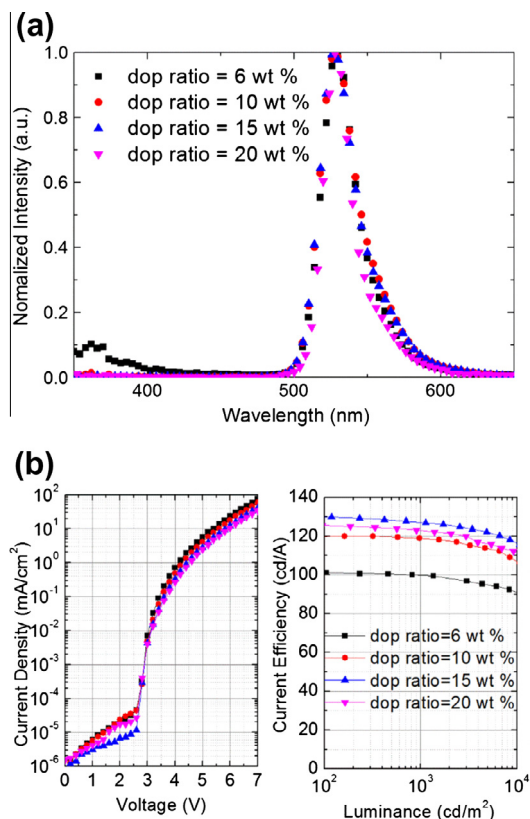


Fig. 7. (a) The normalized EL spectra of different Ir(tfmpppy)₂(tpip) doping ratio, (b) and the current density–voltage (left) and current efficiency–luminance (right) characteristics of different Ir(tfmpppy)₂(tpip) doping ratios.

length unchanged as the MoO₃ thickness increased. As shown in Fig. 6, the current densities of the device become higher when the thickness of MoO₃ layer increases, which may result from better hole injection into EML with either thicker MoO₃ or thinner mCP layer. To identify these two effects, another experiment was conducted, where the

Table 2
Performance parameters of devices with Ir(tfmppy)₂(tpip) doping ratios.

Doping ratio	Turn-on voltage (V)	Max current efficiency (cd/A)	Current efficiency at 10,000 cd/m ² (cd/A)
6%	2.9	101.1 (104.6 cd/m ²)	91.0
10%	2.9	120.0 (162.6 cd/m ²)	107.0
15%	2.9	132.3 (20.4 cd/m ²)	116.3
20%	2.9	126.0 (17.3 cd/m ²)	111.4

mCP layer thickness is unchanged while MoO₃ layer thickness varies. The *I*–*V* characteristics of these devices still show the same trend (data not shown); the thicker MoO₃ layer is, the better *I*–*V* characteristics of device are obtained. Therefore, it is proved that the comparatively thicker MoO₃ can facilitate holes to inject into HTL. However, the current efficiency of the devices decrease significantly as MoO₃ layer thicknesses increase, which is illustrated in the inset of Fig. 6, and it may be attributed to the imbalance of charge carriers, namely, excess injection of holes into light emitting zone.

In the EL spectra of the device C, besides the main peak from the emitter Ir(tfmppy)₂(tpip), some emissions at around 380 nm are still observable, which is attributed to emission from mCP due to incomplete energy transfer from mCP to the emitter, as illustrated in Fig. 4(a). To avoid this issue, we attempted to increase the emitter concentration. A set of devices based on device C with different Ir(tfmppy)₂(tpip) doping concentrations were fabricated, where the doping ratio was set to 6, 10, 15, 20 wt%, respectively. One can see a clear shoulder at around 380 nm for doping ratio of 6 wt% in Fig. 7(a), and with the doping ratio increases, the shoulder peak at 380 nm is suppressed gradually, which suggests that the better energy transfer is realized. The turn-on voltages, maximum current efficiencies, and current efficiency at 10,000 cd/m² of these devices are summarized in Table 2. The current density slightly decreases as the doping concentration increases and the turn-on voltages are almost unchanged, however the current efficiency characteristic behaves significantly different as depicted in Fig. 7(b). The maximum current efficiency of 132.0 cd/A (at the luminance of 20 cd/m²) is obtained when doping ratio is 15 wt%, which results from an effective host-guest energy transfer. Furthermore, an efficiency roll-off as low as around 8.4% is achieved, from 127.0 cd/A at 1000 cd/m² to 116.3 cd/A at 10,000 cd/m². Nevertheless, when the dopant concentration is further increased to 20 wt%, the current efficiency decreases instead, indicating that a serious self-quenching may occur in EML.

4. Summary

In conclusion, the FDTD simulation shows excellent agreement with the experimental data, demonstrating a powerful method for optical optimization in TOLED. A simple top-emitting phosphorescent OLED has been realized with extremely high efficiency and low efficiency roll-off. A maximum efficiency of 132 cd/A is achieved at 20 cd/m², and maintains to 116.3 cd/A at 10,000 cd/m². Moreover, the EL spectra at different viewing angles show

quite weak angular dependence, which is attributed to a properly tuned resonant cavity and a proper antireflection capping layer.

Acknowledgements

This research work was supported by 973 Program (2013CB328803, 2013CB328804), National Natural Science Foundation of China (61377030), Science and Technology Commission of Shanghai Municipal (12JC1404900).

References

- [1] Q. Huang, K. Walzer, M. Pfeiffer, V. Lyssenko, G. He, K. Leo, Highly efficient top emitting organic light-emitting diodes with organic outcoupling enhancement layers, *Appl. Phys. Lett.* 88 (2006) 113515.
- [2] Y. Fan, H. Zhang, J. Chen, D. Ma, Three-peak top-emitting white organic emitting diodes with wide color gamut for display application, *Org. Electron.* 14 (2013) 1898–1902.
- [3] R.M.A. Dawson, M.G. Kane, Pursuit of active matrix organic light emitting diode displays, *SID Int. Symp. Digest Tech. Papers* 32 (2001) 372–375.
- [4] J.J. Lih, C.F. Sung, M.S. Weaver, M. Hack, J.J. Brown, A phosphorescent active-matrix OLED display driven by amorphous silicon backplane, *SID Int. Symp. Digest Tech. Papers* 34 (2003) 14–17.
- [5] S. Hofmann, M. Thomschke, P. Freitag, M. Furno, B. Luessem, K. Leo, Top-emitting organic light-emitting diodes: influence of cavity design, *Appl. Phys. Lett.* 97 (2010) 253308.
- [6] Q. Wang, Y. Tao, X. Qiao, J. Chen, D. Ma, C. Yang, J. Qin, High-performance, phosphorescent, top-emitting organic light-emitting diodes with p–i–n homojunctions, *Adv. Funct. Mater.* 21 (2011) 1681–1686.
- [7] A. Chutinan, K. Ishihara, T. Asano, M. Fujita, S. Noda, Theoretical analysis on light-extraction efficiency of organic light-emitting diodes using FDTD and mode-expansion methods, *Org. Electron.* 6 (2005) 3–9.
- [8] M.A. Baldo, D.F. O'Brien, Y. You, A. Shoustikov, S. Sibley, M.E. Thompson, S.R. Forrest, Highly efficient phosphorescent emission from organic electroluminescent devices, *Nature* 395 (1998) 151–154.
- [9] Y. Kawamura, K. Goushi, J. Brooks, J.J. Brown, H. Sasabe, C. Adachi, 100% phosphorescence quantum efficiency of Ir(III) complexes in organic semiconductor films, *Appl. Phys. Lett.* 86 (2005) 071104.
- [10] M.A. Baldo, C. Adachi, S.R. Forrest, Transient analysis of organic electrophosphorescence. II. Transient analysis of triplet–triplet annihilation, *Phys. Rev. B* 62 (2000) 10967–10977.
- [11] E. Najafabadi, K.A. Knauer, W. Haske, C. Fuentes-Hernandez, B. Kippelen, Highly efficient inverted top-emitting green phosphorescent organic light-emitting diodes on glass and flexible substrates, *Appl. Phys. Lett.* 101 (2012) 023304.
- [12] E. Najafabadi, K.A. Knauer, W. Haske, B. Kippelen, High-performance inverted top-emitting green electrophosphorescent organic light-emitting diodes with a modified top Ag anode, *Org. Electron.* 14 (2013) 1271–1275.
- [13] Y.-C. Zhu, L. Zhou, H.-Y. Li, Q.-L. Xu, M.-Y. Teng, Y.-X. Zheng, J.-L. Zuo, H.-J. Zhang, X.-Z. You, Highly efficient green and blue-green phosphorescent OLEDs based on iridium complexes with the tetraphenylimidodiphosphinate ligand, *Adv. Mater.* 23 (2011) 4041–4046.
- [14] J. Lee, J.-I. Lee, K.-I. Song, S.J. Lee, H.Y. Chu, Effects of interlayers on phosphorescent blue organic light-emitting diodes, *Appl. Phys. Lett.* 92 (2008) 203305.
- [15] Z. Liu, M.G. Helander, Z. Wang, Z. Lu, Highly efficient two component phosphorescent organic light-emitting diodes based on direct hole injection into dopant and gradient doping, *Org. Electron.* 14 (2013) 852–857.
- [16] X.-W. Chen, W.C.H. Choy, S. He, P.C. Chui, Comprehensive analysis and optimal design of top-emitting organic light-emitting devices, *J. Appl. Phys.* 101 (2007) 113107.
- [17] E.D. Palik, *Handbook of Optical Constants of Solids*, Academic, Orlando, 1985.
- [18] R.A. Synowicki, Spectroscopic ellipsometry characterization of indium tin oxide film microstructure and optical constants, *Thin Solid Films* 313–314 (1998) 394–397.
- [19] P.K. Raychaudhuri, J.K. Madathil, J.D. Shore, S.A. Van Slyke, Performance enhancement of top- and bottom-emitting organic

- light-emitting devices using microcavity structures, *J. Soc. Inf. Display* 12 (2004) 315–321.
- [20] J. Wang, J. Liu, S. Huang, X. Wu, X. Shi, G. He, Y. Zheng, Improved efficiency roll-off at high brightness in simplified phosphorescent organic light emitting diodes with a crossfading-host, *Org. Electron.* 14 (2013) 2682–2686.
- [21] Y. Chen, J. Chen, Y. Zhao, D. Ma, High efficiency blue phosphorescent organic light-emitting diode based on blend of hole- and electron-transporting materials as a co-host, *Appl. Phys. Lett.* 100 (2012) 213301.
- [22] J. Wang, J. Liu, S. Huang, X. Wu, X. Shi, C. Chen, Z. Ye, J. Lu, Y. Su, G. He, Y. Zheng, High efficiency green phosphorescent organic light-emitting diodes with a low roll-off at high brightness, *Org. Electron.* 14 (2013) 2854–2858.